# Time-resolved study of the crystallization dynamics in a metallic glass

Michael Leitner,[*] Bogdan Sepiol, and Lorenz-Mathias Stadler[†]
*Universität Wien, Fakultät für Physik, Strudlhofgasse 4, 1090 Wien, Austria*

Bastian Pfau
*TU Berlin, Institut für Optik und Atomare Physik, Hardenbergstraße 36, 10623 Berlin, Germany*
(Received 26 March 2012; revised manuscript received 11 May 2012; published 7 August 2012)

We report a study of the atomic-scale dynamics in a metallic glass of composition $Zr_{65}Ni_{10}Cu_{17.5}Al_{7.5}$ by x-ray photon correlation spectroscopy. Our results show a continuous slowing down of the dynamics from the pristine state of the sample until crystallization. We propose a phenomenological model in a framework of thermally activated dynamics with a decreasing attempt rate dependent on the sample state that quantitatively describes our results, giving an activation energy of $E_A = 1.95 \pm 0.10$ eV. This allows us to conclude that atomic motion and crystallization are manifestations of the same process, with the time scale of crystallization on the order of 100 local atomic rearrangements. This rules out the notion of equilibrium diffusion in a relaxed glassy state in this system.

DOI: 10.1103/PhysRevB.86.064202 PACS number(s): 66.30.hh, 64.70.dg, 61.05.cf, 81.05.Kf

## I. INTRODUCTION

For metallic systems in their conventional form, the crystalline phase, there is often a large gap between the theoretical and the actual values of parameters of technical importance, e.g., tensile strength or corrosion resistance. This is for the most part due to the unavoidable imperfections of the crystalline order such as grain boundaries, which are weak spots where cracks or corrosion can begin to degrade the integrity of the sample. Amorphous metals, on the other hand, are a very promising class of materials from this perspective.[1] They have no grain boundaries, so the actual mechanical strengths are close to their theoretical values, and due to the stability of the amorphous phase, it is also much harder for the corroding agents to make inroads.

Preparing a metallic sample in the amorphous state is in principle not difficult. If a melt is cooled rapidly enough, the atoms do not have enough time to arrange in a crystal lattice and become frozen in the amorphous state. Due to the requirement of a high cooling rate, the achievable size of the amorphous samples is limited, however. In recent years, an ever-increasing number of systems has been discovered, where the necessary cooling rates allow the preparation of bulk samples. These are the so-called bulk metallic glasses, due to the above reasons one of the main emerging fields in materials science. With the invention of sophisticated processing techniques, their industrial application seems imminent.[2] Bulk metallic glasses consist in most cases of three or more components, and while they often share a typical majority component (such as Zr or Pd), the stability of the amorphous phase at a given composition can still only be ascertained experimentally.

The excess free enthalpy of the amorphous phase compared to the crystalline ground state is the driving force leading to crystallization at elevated temperatures. Apart from the difference in free enthalpy, the crystallization rate is governed by atomic motion. In contrast to the case of crystalline media, where diffusion happens as a rule via thermal vacancies, in metallic glasses the situation is not so clear (see, e.g., Refs. 3 and 4 for a review). The predominant view is that here diffusion is mediated by highly collective processes, involving tens of atoms,[5,6] but it has also been proposed that just as in crystals, the random motion of less dense regions, termed quasivacancies, is responsible for mass transport.[7,8] The calorimetric glass transition seems to be connected to a change in the dynamics[9] and, moreover, it is well conceivable that different mechanisms are responsible for the diffusion of the respective constituents.[10]

The main experimental method for measuring diffusion is the radiotracer method. This method measures the spreading out of concentration gradients of radioactive isotopes and directly gives the diffusion constant, which is a macroscopic quantity. However, detailed information on the diffusive processes on their fundamental scale, i.e., how the atoms move, can only be inferred indirectly, for example through measurements of the isotope effect[8,11] or the pressure dependence.[12,13] First-hand information on the processes on the atomic scale would therefore be highly desirable. Such information can be obtained by atomistic methods such as quasi-elastic neutron scattering (QENS). This method has been applied successfully for the study of melts,[14] but it can not resolve the very slow relaxations in solid metallic glasses.

Conversely, relaxations on the time scale of minutes to hours are the natural domain for the recently established method of atomic-scale x-ray photon correlation spectroscopy (aXPCS),[15,16] which can be seen as the x-ray counterpart of QENS in the time domain. It works by scattering coherent x-rays at the sample and correlating over time the fluctuations in the scattered radiation at wave-vector transfers corresponding to atomic distances. Diffusivities as low as $10^{-23}$ $m^2$ $s^{-1}$ can be resolved, corresponding to less than 10 atomic jumps during the experiment. As such, it is the most powerful method for studying slow diffusive dynamics in solids. Here, we employ this method for the first direct experimental investigation of the atomic-scale dynamics in a metallic glass, in our case the Inoue alloy[17] $Zr_{65}Ni_{10}Cu_{17.5}Al_{7.5}$.

As metallic glasses are not strictly in thermodynamic equilibrium, their state is not only a function of the instantaneous temperature, but also of their preparation and subsequent thermal history. At intermediate temperatures, high enough

 

for atomic motion in the sample to happen, but before rapid crystallization or melting sets in, the sample will relax towards regions in phase space with lower free enthalpy. It is intuitive that this leads to an increase in density, and a concomitant slowing-down of diffusion due to the decrease of free volume. Such effects have indeed been observed.[11] It is conventionally claimed, however, that eventually the sample reaches a relaxed state with a steady diffusion rate, and that therefore the notion of a (metastable) equilibrium diffusion rate in the amorphous state at a given temperature is well defined (see, e.g., Ref. 18). The present experimental evidence for this assumption is only indirect, however, as in tracer experiments the instantaneous diffusion rate can not be ascertained, only the integrated squared translation. Here, we reexamine this issue critically by monitoring the instantaneous dynamics during annealing by aXPCS, which, being a scattering method, gives also a convenient gauge on the progress of crystallization. We show that in the present case the atoms can not diffuse more than a few nanometers until crystallization sets in, subject to a steady slowing down of dynamics, which contradicts the notion of equilibrium diffusion in the amorphous state, and we give a phenomenological theory to describe our results.

## II. EXPERIMENTAL METHOD

### A. Theory

Photon correlation spectroscopy, also called dynamic light scattering, has been a popular method for studying diffusive dynamics at length scales of micrometers in liquids since the 1960s.[19] As any scattering experiment, it utilizes the connection between the scatterer density in the sample and the scattering amplitude via the Fourier transform. In contrast to most other scattering methods, where incoherent illumination leads to smooth scattering patterns that bear only information on the macroscopic state of the sample, here this equivalence holds in a strict sense without any averaging taking place due to the coherent illumination as provided by, e.g., lasers. The scattered intensity therefore shows modulations in reciprocal space on the scale of the inverse of the dimensions of the illuminated volume, known as speckles, which are directly related to the microscopic configuration of the sample. Dynamics lead to a temporal evolution of the speckle pattern. This can be quantified by computing the intensity autocorrelation function

$$g^{(2)}(\Delta t,\vec{q}) = \frac{\langle I(.,\vec{q})I(.+\Delta t,\vec{q})\rangle}{\langle I(.,\vec{q})\rangle^2}, \qquad (1)$$

where $I(t,\vec{q})$ is the intensity scattered at time $t$ into the direction corresponding to wave-vector transfer $\vec{q}$, corrected for fluctuations in the incoming intensity. The value of $g^{(2)}(\Delta t,\vec{q})$ for a distinct $\Delta t$ gives the correlation between intensities separated by a time delay of $\Delta t$, where a value of 1 corresponds to no correlations and higher values to nonvanishing correlations.

With the availability of sufficient coherent x-ray intensity, this technique has been extended to the study of dynamics at ranges of tens of nanometers,[20–22] but only recently it has become possible to follow dynamics on the scale of atomic distances.[15,23]

The high wave-vector transfers that are necessary in atomic-scale XPCS entail high demands on the coherence of the beam, which, together with the low scattering efficiency in the diffuse range, leads to low count rates at the detector. It is therefore necessary to use a multipixel detector, which allows us to perform the average in Eq. (1) over both absolute time and the pixels of the detector. With this approach it is possible to measure dynamics with correlation times that are on the order of the experimental duration. It is necessary, however, to account for the effects of intensity gradients over the detector, which would artificially raise the value of $g^{(2)}(\Delta t,\vec{q})$ above unity even in the absence of correlations.

The conventional interpretation of an XPCS experiment is in terms of van Hove's pair correlation function[24,25] $G(\Delta\vec{x},\Delta t)$, which is the spatiotemporal correlation function of the electron density or, equivalently, the conditional probability for an electron to be found at a position $\vec{x}+\Delta\vec{x}$ and a time $t+\Delta t$ given that there was an electron at position $\vec{x}$ at time $t$. By appropriate rescaling, this electronic pair-correlation function directly translates to the atomic pair-correlation functions. A spatial Fourier transform of the pair-correlation function gives the amplitude autocorrelation function $g^{(1)}(\Delta t,\vec{q})$, which in turn is connected to the intensity autocorrelation function $g^{(2)}(\Delta t,\vec{q})$ via the so-called Siegert relation.[26] One therefore explains the features observed in the measured $g^{(2)}(\Delta t,\vec{q})$ by formulating models in real space and deciding between them by how well they fit the data.

### B. Sample

The sample was prepared in the glassy state by melt spinning as described in Ref. 27. The extrapolated quasistationary glass transition is given at about 330 °C. Thin foils for the experiment in transmission geometry were obtained by subjecting ribbons of the material to cold rolling, without any additional temperature treatment. Note that the cold rolling gives also a well-defined and reproducible sample state in contrast to the hardly controllable local cooling rates in melt spinning. The actual thickness at the measurement position could be determined very accurately via the measured transmission for 8 keV photons, giving a value of 11 $\mu$m.

Figure 1 shows the x-ray diffraction curve of the sample after rolling, immediately before the start of the XPCS

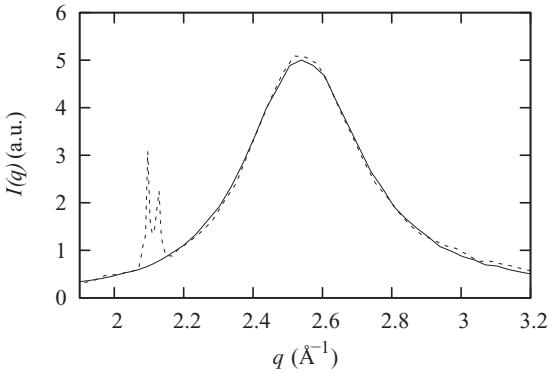


FIG. 1. X-ray diffraction curve of the sample before (solid) and after the experiment (dashed) obtained at the same position. The sharp peaks at smaller $q$ show the emerging of crystalline intermetallic phases. For the experiment, the detector was positioned in the glass peak at $q = 2.58$ Å$^{-1}$.

experiment. It shows the generic features of a glass, a well-defined peak corresponding to a nearest-neighbor distance of about 2.4 Å with a width of about 10%. The diffraction curve obtained after the experiment clearly demonstrates that there has been nucleation of crystalline intermetallic phases during the experiment. The diffraction curve has been taken with the collimated beam and a point detector, therefore information on the relative amount of the crystalline phase in the sample can be inferred only with large uncertainties due to the spatially inhomogeneous nature of nucleation. Still, it is evident that the time and temperature ranges explored during the experiment cause the onset of crystallization in the sample.

### C. Setup

We performed the experiment at beamline ID10A at the European Synchrotron Radiation Facility in Grenoble, France. The x-ray beam was focused with a Be compound refractive lenses system. We used a photon energy of 8.0 keV (wavelength 1.55 Å), monochromatized by a Si-(111) monochromator with an energy resolution of $\Delta E/E = 1.4 \times 10^{-4}$ ensuring temporal coherence. The beam was cut to $7 \times 7\ \mu\text{m}^2$ by movable slits 15 cm upstream of the sample. The vacuum furnace was directly connected to the flight tube, with Kapton foil sealing both the furnace's entrance window and the flight tube's exit window. The sample foil was mounted in transmission geometry. The sample holder was resistively heated with a temperature stability within 0.1 K. From experience with similar furnaces, we estimate the systematic bias between nominal and actual temperature of the sample to be less than 10 K. The thermal latency of the furnace was such that, after changing the target temperature by a few tens of degrees, it took about 2 min for the furnace to reach the new value and about 10 min to settle there. The scattered radiation was detected using a direct-illumination charge-coupled device (CCD) camera (Princeton Instruments, $1340 \times 1300$ pixels, $20 \times 20\ \mu\text{m}^2$ pixel size). The camera was placed 1.32 m from the sample, where the corresponding pixel solid angle constitutes a compromise between gaining scattered intensity without losing too much contrast.

### D. Data evaluation

Series of frames with 5 s exposure per frame and typically 2 h duration were taken. Due to read-out time, this gives one frame per 7.36 s. The data were subjected to the so-called droplet algorithm,[16,28] which detects single 8.0 keV photon events within these frames. This serves a threefold purpose: it greatly reduces the overall computing time and makes it possible to compute the autocorrelation function incrementally online, background noise and fluorescence are suppressed, and it allows us to compute the expected standard deviations of the points in the autocorrelation function in absolute values by basic probability theory. The count rates were typically 3 photons per hour and pixel. As the variation in $q$ over the detector was only 3%, all the pixels were treated as equivalent for computing the average in the autocorrelation function. There was a minimal variation of the mean intensity over the detector, for which the computed auto-correlation functions were corrected.

## III. RESULTS

We studied the influence of the sample temperature on the observed dynamics over the course of about 36 h, at temperatures both above and below the glass temperature. We accurately recorded the temperatures and durations of the annealing steps in order to correlate the evolution of the instantaneous dynamics with the heat treatment. All measurements were done in the intensity maximum due to short-range order at a scattering angle of $2\theta = 37^\circ$, corresponding to $q = 2.58\ \text{Å}^{-1}$. We want to note that these values correspond to the smallest real-space length scales reported for a photon correlation experiment so far.

### A. Autocorrelation functions

A representative measured autocorrelation function is given in Fig. 2. Due to the demanding requirements on the coherence of the illumination and the concomitant very low number of detected photons, statistical scatter in the data points can be seen. It is clear, however, that the form of the autocorrelation function does not correspond to a simple exponential decay as predicted by random-walk theory. It can be fitted instead by a so-called compressed exponential decay

$$g^{(2)}(\Delta t) = 1 + \beta \exp[-(\Delta t/\tau)^{\gamma}], \tag{2}$$

which is a phenomenological model for a behavior often found in disordered media.[29–32] The fitted compressing exponents $\gamma$ varied around the value of 2 with a standard deviation of about 0.3, with no systematic variation with temperature or time. The coherence factors $\beta$ were about 2%. This low value is due to the difficulty of fulfilling the requirement of coherence at high scattering vectors. Still, the correlation time can be determined very accurately, for the fit reported in Fig. 2 it is $754 \pm 25$ s.

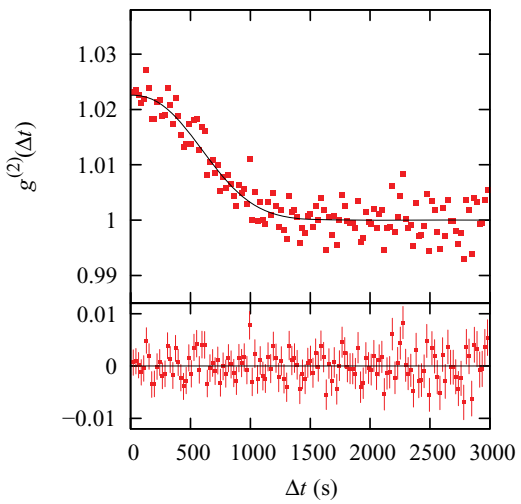


FIG. 2. (Color online) Initial part of an exemplary intensity autocorrelation function, measured at 340 °C around time $t = 20$ h (see Fig. 3) together with a fitted compressed exponential decay (upper part). The residuals (lower part) show the validity of the fit, with a reduced $\chi^2 = 0.9922$ at 815 degrees of freedom.

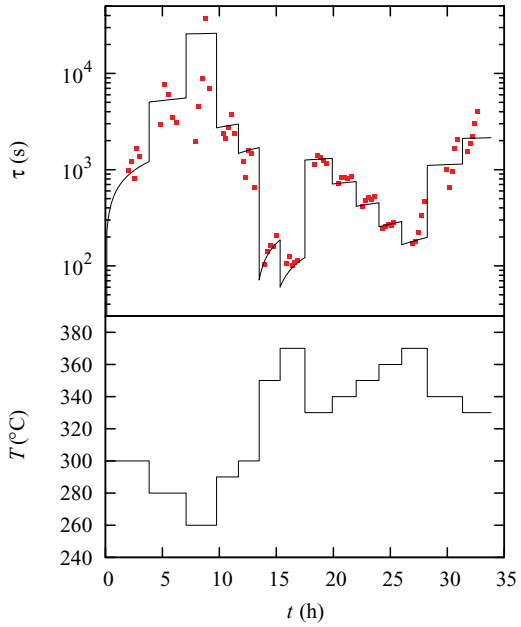


FIG. 3. (Color online) Temperature of the sample over the course of the experiment (lower plot) and instantaneous correlation times (upper plot) over the course of the experiment. For the fitted temperature/time dependence (solid line in upper plot), see Sec. IV.

### B. Temporal evolution of correlation times

In order to gain more information about the temporal evolution of the dynamics, we turned to a more involved evaluation procedure. Instead of computing and fitting the autocorrelation function over all frames from a temperature step (on the order of 800), we computed the autocorrelation function over subranges of the frames. To be specific, we divided the set of frames for a given temperature step into six equal parts and computed the autocorrelation functions for each of the five ranges of two successive parts. As the coherence factor $\beta$ depends only on the setup but not on the sample, we used a fixed value of 2% for fitting. We also fixed the compressing exponent $\gamma$ in the cases where the correlation times were longer than the time delays covered by the autocorrelation function. Figure 3 shows the sequence of temperatures and the evolution of the correlation times for each temperature step. The thermal latency is neglected.

### C. Data noise

An XPCS experiment (the following arguments pertain to optical PCS as well) consists essentially in detecting the temporally decreasing agreement in the scattering pattern due to a dynamical evolution of the sample. Since instabilities of either the illumination, the sample, or the detector lead to an additional loss of correlation, the experimental method poses strict requirements on the stability of the setup. As a consequence, the maximum detectable time scales in an XPCS experiment are determined by the degree of stability of the setup: if the dynamics of the sample are fast, correlations in the scattering patterns have vanished long before instabilities of the setup can have detrimental effects. Thus, the fitted correlation time is determined only by the sample dynamics. On the other hand, if the sample dynamics is slow, the measured decay of the autocorrelation function will be due to the instabilities of the setup and will likely display a noisy behavior due to sudden movements.

The above arguments help to understand the measured correlation times reported in Fig. 3. At high temperatures, the correlation times are short and, consequentially, scatter only weakly. The noise in the data points for the slow dynamics at low temperatures suggests that the longest accurately detectable correlation times are on the order of a few thousands of seconds. In principle, there are two possible reasons for this noise: either instabilities in the setup, i.e., the beam, the sample environment, or the detector, occur on the observed time scales, or the sample itself features intrinsic stochastic processes. Based on measurements on single crystals (as reported in Ref. 15, but also in other yet unpublished measurements) taken at the same beamline using the same sample environment even during the same beamtime period, we are able to exclude setup instabilities causing the loss in correlation since we never observed such instabilities on the relevant time scales. Therefore, we have rather come to the conclusion that these instabilities originate from the sample and are a consequence of the inherently unstable nature of the metallic glass, which has been corroborated by additional test measurements during subsequent beamtimes. It is conceivable that, e.g., the stochasticity of nucleation of crystalline phases with the concomitant large-scale strains due to the volume change gives rise to these effects.

## IV. INTERPRETATION

Despite the precautionary argumentation above, the information content of the results in Fig. 3 is obvious: the effect of temperature on the correlation times is undisputable. Apart from this effect, also the slowing down of the dynamics with time is evident. A later measurement at a given temperature systematically gives longer correlation times than an earlier measurement at the same temperature. Furthermore, also within one temperature step the correlation times get progressively longer, which is especially visible at high temperatures and accordingly short correlation times. We interpret this finding as an indication of a progressive structural relaxation of the glass to a state of higher order and therefore lower rearrangement frequencies.

We will now develop a phenomenological model to describe our results. It is accepted that equilibrium diffusivity data can be well described by an Arrhenius dependence in a wide class of systems, at least over a limited temperature range. This formulation employs two parameters: the prefactor and the activation enthalpy. In order to describe our observations, i.e., an evolution of the state of the sample over time, at least one additional parameter, which gives the time scale of the relaxation, is needed in the simplest case.

We assume that the dynamics as measured by XPCS is responsible for the relaxation, and therefore relaxation is fast when the measured dynamics is fast. We therefore formulate our model with a correlation time $\tau(T,t)$ following an Arrhenius dependence

$$\tau(T,t) = \tau_0(t) e^{E_A/k_B T}, \tag{3}$$

but with an attempt time $\tau_0(t)$ that grows in time, where the growth rate is proportional to the instantaneous dynamics

$$\frac{d}{dt}\tau_0(t) = \frac{\alpha}{\tau(T,t)}. \quad (4)$$

In this formulation, the current state of the sample is described by the attempt time $\tau_0(t)$.

Solving this system of ordinary differential equations for a constant temperature gives

$$\tau_0(t) = \sqrt{2\alpha e^{-E_A/k_B T}(t - t_0) + \tau_0(t_0)^2}. \quad (5)$$

From this equation it follows that annealing the sample at a given temperature for a given time results in a growth of the square of the attempt time that is independent of the actual value of the attempt time. Therefore, the relaxation of the sample achieved after a number of temperature steps of given durations is independent of the order of the temperature steps.

To construct the evolution of $\tau_0(t)$ over the course of the experiment, we used Eq. (5) during a period of constant temperature and took the resulting final $\tau_0$ at this temperature as the starting value for the next period, so that the resulting evolution of $\tau_0$ is continuous and monotonically increasing.

The instantaneous correlation times $\tau(T,t)$ obtained with the parameters $E_A = 1.95$ eV, $\alpha = 4 \times 10^{-16}$ s, and an initial value of the attempt time $\tau_0$ equal to zero are plotted in the upper panel of Fig. 3. This choice of the growth rate factor $\alpha$ results in a 12-fold increase of the attempt time $\tau_0(t)$ from the end of the first to the end of the last temperature step. Due to the possibility that especially the correlation times measured at temperatures below 300 °C are compromised by instabilities of the setup, deviations of the measured correlation times towards lower values are much more probable than towards higher values, which was taken into account during fitting. The accuracy of the determined activation energy is estimated to be 0.1 eV.

The fit between our model and the experimental data is very satisfactory both in a qualitative and in a quantitative sense: It describes the growth of the correlation times (i.e., the slowing down of dynamics) both between measurements at the same temperature at different times and within one temperature step. Also, the values of the correlation times for the higher temperatures fit very accurately; only very long correlation times are underestimated. This is an indication of instabilities of the setup as discussed above, and places the longest measurable time scales on the order of an hour. The fact that even the quantitative description of the slowing down of dynamics is good verifies our assumption that the state of the sample is described by a single parameter (within our experimental resolution) that corresponds to a monotonous slowing down, as opposed to, e.g., transient relaxations towards the new equilibrium state after each temperature step as observed in intermetallics.[33]

The predominant microscopic picture of atomic rearrangements in a metallic glass is as follows: There is not one defined transition responsible for atomic mass transport, but rather the multitude of atomic-scale arrangements is reflected in the number of possible transitions, corresponding to a distribution of activation energies. For low temperatures, only the low-energy tail of this distribution is active, which consists of transitions involving a large number of atoms performing correlated movements, therefore low jump entropies and low attempt frequencies. There are two extreme points of view on the slowing down of dynamics due to relaxation:

(i) In an unrelaxed glass, there are arrangements that allow low-energy transitions. After such a transition, the local configuration energy is much lower (in the extreme case the sample has locally crystallized), as a consequence a further rearrangement would need a much higher activation energy and is practically forbidden. Relaxation consists therefore in the annealing of the possibilities of low-energy transitions.

(ii) Relaxation proceeds via a gradual increase of local order and therefore in an increase in the activation energies, while the complexity of the transitions stays roughly constant.

The model that we use to describe our data, which assumes constant activation energy and growing attempt time, corresponds to the former view. We do not claim, however, that this is a clear indication on the validity of one view or the other. We rather chose this formulation mainly for aesthetical reasons, as it allows us to solve the differential equation governing the evolution of the instantaneous correlation time analytically and to describe the totally unrelaxed state by an attempt time of zero. In reality, however, relaxation will most probably lead to an increase of both activation energies and complexity of the transitions, corresponding to growing attempt times.

The question of the nature of the observed dynamics has been left open up to now. Especially the compressed exponential decay of the measured autocorrelation function, which is at odds with a picture of atoms performing uncorrelated random walks without memory, independent of each other, deserves closer attention. Such phenomena have been observed in soft matter by both optical and x-ray PCS,[29–32] and mechanisms explaining the shapes in terms of the decay of stresses in the sample,[34] ballistic motion,[31] or just by invoking the so-called "jamming" transition,[35] have been put forward. These theories are obviously not immediately transferable to the case of metallic glasses, rather one could speculate about the effects of the buildup of stresses due to the nucleation of the crystalline phase on the autocorrelation function. A more thorough investigation into this question will be the subject of a later publication.

The measured correlation times are the decay times of the Fourier component of the electrons' pair-correlation function at the short-range order peak. It therefore gives the time scale of the evolution of the electron density fluctuations on atomic length scales. However, apart from the usual interpretation of XPCS measurements in terms of local diffusive dynamics, i.e., random displacements of the atoms, also macroscopic translations, rotations, or strain of the sample as a whole lead to a temporal evolution of the electron density and therefore to a decay of the measured autocorrelation function. The converse argument is strictly valid, however: On time scales over which the autocorrelation function shows no decay, there is no diffusion.

To get a feel of the effects we induced in the sample by the temperature treatment, we observe that our probed wavevector transfer $q$ corresponds to the nearest-neighbor distance of $d = 2.4$ Å, and therefore the inverse of the instantaneous correlation time is a gauge of the atomic-scale rearrangement frequency. Integrating this frequency over time gives the number of such rearrangements, which in our case evaluates to 280 during the whole experiment. The resulting diffusive

root-mean-square displacement is therefore $d\sqrt{280} = 4$ nm under the assumption that the observed dynamics leads to diffusive mass transport, or even less when not. As shown above, after this temperature treatment the onset of crystallization is evident.

The parameters of our model deserve further discussion: The activation energy, as in any thermally activated process, determines via the Boltzmann factor how much the dynamics gets faster under a given step in temperature. Its fitted value of $E_A = 1.95 \pm 0.10$ eV is in the same range as activation energies for diffusion in crystalline metals,[36] but actually also compares very well to the value of $E_A = 2.16 \pm 0.13$ eV obtained for Ni-tracer diffusion in this metallic glass and temperature range.[37]

The meaning of the growth rate parameter $\alpha = 4 \times 10^{-16}$ s can also be translated into common concepts: Due to our model, the prefactor grows by $\alpha$ during one correlation time, i.e., during one atomic jump. As the number of jumps during the experiment is on the order of hundreds, this gives a prefactor in Eq. (3) on the order of $10^{-13}$ s or an attempt frequency of $10^{13}$ $s^{-1}$, which again is in the range known from diffusion in crystals.[36]

## V. CONCLUSIONS

To conclude, we reported an aXPCS measurement on a metallic glass at temperatures around the glass transition. The time and temperature ranges probed here correspond to displacements on the order of a few nanometers, during which the sample evolves from the pristine state to the onset of crystallization. The autocorrelation functions show a compressed exponential decay. We directly obtained the instantaneous dynamics in real time from the measured correlation times. These exhibit a progressive slowing down, concurrent to the onset of crystallization, which we interpret as a continuous relaxation of the system towards the crystalline ground state.

We derived a basic phenomenological theory which can describe our experimental results very well both qualitatively and quantitatively with two fitted parameters. The activation enthalpy of $E_A = 1.95 \pm 0.10$ eV is in good agreement with results obtained by tracer measurements.[37] However, the fit between our experimental results and our theory shows that atomic mobility and crystallization do not happen independently of each other. Additionally, only on the order of 100 atomic rearrangements happen during the transition from a pristine sample to a state showing clear signs of crystallization. These observations rule out the concept of equilibrium diffusion in a well-defined relaxed amorphous state of the sample, as put forward in numerous tracer diffusion measurements,[7,18] at least in the present example of a bulk metallic glass.

We have shown here that atomic-scale XPCS is a viable method to investigate the instantaneous dynamics on the atomic scale directly *in real time*, which makes it possible to draw detailed conclusions on the fundamental mechanisms in nonequilibrium processes.

## ACKNOWLEDGMENTS

We thank A. Meyer (TU München, Physik-Department E13) for providing the sample. This work was supported by the Austrian Science Fund (FWF): P22402.

*Now at Forschungsneutronenquelle Heinz Maier-Leibnitz (FRM-II), Technische Universität München, Lichtenbergstraße 1, 85747 Garching, Germany; michael.leitner@frm2.tum.de

†Now at Kliment, and Henhapel Patentanwälte OG, Singerstraße 8/9, 1010 Wien, Austria.

[1] *Bulk Metallic Glasses*, edited by M. Miller and P. K. Liaw (Springer, New York, 2008).

[2] W. L. Johnson, G. Kaltenboeck, M. D. Demetriou, J. P. Schramm, X. Liu, K. Samwer, C. P. Kim, and D. C. Hofmann, Science **332**, 828 (2011).

[3] F. Faupel, W. Frank, M. P. Macht, H. Mehrer, V. Naundorf, K. Rätzke, H. R. Schober, S. K. Sharma, and H. Teichler, Rev. Mod. Phys. **75**, 237 (2003).

[4] F. Faupel and K. Rätzke, in *Diffusion in Condensed Matter*, 2nd ed., edited by P. Heitjans and J. Kärger (Springer, Berlin, 2005), pp. 249–282.

[5] K. Rätzke, V. Zöllmer, A. Bartsch, A. Meyer, and F. Faupel, J. Non-Cryst. Solids **353**, 3285 (2007).

[6] H. Ehmler, A. Heesemann, K. Rätzke, F. Faupel, and U. Geyer, Phys. Rev. Lett. **80**, 4919 (1998).

[7] W. Frank, J. Horváth, and H. Kronmüller, Mater. Sci. Eng. **97**, 415 (1988).

[8] K. Rätzke, P. W. Hüppe, and F. Faupel, Phys. Rev. Lett. **68**, 2347 (1992).

[9] X. P. Tang, U. Geyer, R. Busch, W. L. Johnson, and Y. Wu, Nature (London) **402**, 160 (1999).

[10] U. K. Rößler and H. Teichler, Phys. Rev. E **61**, 394 (2000).

[11] H. Ehmler, K. Rätzke, and F. Faupel, J. Non-Cryst. Solids **250–252**, 684 (1999).

[12] P. Klugkist, K. Rätzke, S. Rehders, P. Troche, and F. Faupel, Phys. Rev. Lett. **80**, 3288 (1998).

[13] K. Knorr, M.-P. Macht, K. Freitag, and H. Mehrer, J. Non-Cryst. Solids **250–252**, 669 (1999).

[14] A. Meyer, J. Wuttke, W. Petry, O. G. Randl, and H. Schober, Phys. Rev. Lett. **80**, 4454 (1998).

[15] M. Leitner, B. Sepiol, L.-M. Stadler, B. Pfau, and G. Vogl, Nat. Mater. **8**, 717 (2009).

[16] M. Leitner, *Studying Atomic Dynamics with Coherent X-rays* (Springer, Berlin, 2012).

[17] A. Inoue, in *Materials Science Forum*, Vols. 179–181 (Trans Tech Publications, Zurich, 1995), pp. 691–700.

[18] W. Frank, in *Defect and Diffusion Forum*, Vol. 143 (Trans Tech Publications, Zurich, 1997), pp. 695–710.

[19] *Dynamic Light Scattering: The Method and Some Applications*, edited by W. Brown (Clarendon, Oxford, 1993).

[20] S. Brauer, G. B. Stephenson, M. Sutton, R. Brüning, E. Dufresne, S. G. J. Mochrie, G. Grübel, J. Als-Nielsen, and D. L. Abernathy, Phys. Rev. Lett. **74**, 2010 (1995).

[21] S. B. Dierker, R. Pindak, R. M. Fleming, I. K. Robinson, and L. Berman, Phys. Rev. Lett. **75**, 449 (1995).
[22] B. Pfau, L.-M. Stadler, B. Sepiol, R. Weinkamer, J. W. Kantelhardt, F. Zontone, and G. Vogl, Phys. Rev. B **73**, 180101 (2006).
[23] M. Leitner and G. Vogl, J. Phys.: Condens. Matter **23**, 254206 (2011).
[24] F. Zernike and J. A. Prins, Z. Phys. **41**, 184 (1927).
[25] L. van Hove, Phys. Rev. **95**, 249 (1954).
[26] A. J. F. Siegert, Radiation Laboratory Report No. 465, 1943, Massachusetts Institute of Technology (unpublished).
[27] A. Meyer, J. Wuttke, W. Petry, A. Peker, R. Bormann, G. Coddens, L. Kranich, O. G. Randl, and H. Schober, Phys. Rev. B **53**, 12107 (1996).
[28] F. Livet, F. Bley, J. Mainville, R. Caudron, S. G. J. Mochrie, E. Geissler, G. Dolino, D. Abernathy, G. Grübel, and M. Sutton, Nucl. Instrum. Methods Phys. Res., Sect. A **451**, 596 (2000).
[29] L. Cipelletti, S. Manley, R. C. Ball, and D. A. Weitz, Phys. Rev. Lett. **84**, 2275 (2000).
[30] P. Falus, M. A. Borthwick, S. Narayanan, A. R. Sandy, and S. G. J. Mochrie, Phys. Rev. Lett. **97**, 066102 (2006).
[31] C. Caronna, Y. Chushkin, A. Madsen, and A. Cupane, Phys. Rev. Lett. **100**, 055702 (2008).
[32] A. Madsen, R. L. Leheny, H. Guo, M. Sprung, and O. Czakkel, New J. Phys. **12**, 055001 (2010).
[33] R. Kozubski and W. Pfeiler, Acta Mater. **44**, 1573 (1996).
[34] J. Bouchaud and E. Pitard, Eur. Phys. J. E **6**, 231 (2001).
[35] A. J. Liu and S. R. Nagel, Nature (London) **396**, 21 (1998).
[36] H. Mehrer, *Diffusion in Solids: Fundamentals, Methods, Materials, Diffusion-Controlled Processes* (Springer, Berlin, 2007).
[37] K. Knorr, Ph.D. thesis, Universität Münster, 1999.